LA-UR-21-23240
Approved for public release; distribution is unlimited.

Title: Estimating Beam-Target Heating

Author(s): Ekdahl, Carl August Jr.

Intended for: Report

Issued: 2021-04-05

# Estimating Beam-Target Heating

Carl Ekdahl

## I. INTRODUCTION

At Los Alamos National Laboratory, two high-current linear induction accelerators (LIAs) are used to produce bremsstrahlung source spots for flash radiography of high-explosive driven hydrodynamic experiments at the Dual Axis Radiographic Hydrodynamic Test (DARHT) facility [1, 2]. Measurements of the electron-beam current density profile are valuable for understanding the beam dynamics in order to improve the quality of the radiography source spot. A technique commonly used at DARHT is to image the profile in Cerenkov or Optical Transition Radiation (OTR) light created by the beam striking a thin target inserted into the beam line [3, 4]. Target materials include aluminized dielectrics and titanium foils for OTR, and fused silica wafers for Cerenkov radiation.

A practical complication with this technique is heating of the target by the electron beam. If the beam density is too great, the target can be destroyed. Moreover, even if the beam density is kept low enough to be nondestructive, the beam can heat the target to a high enough temperature to desorb gas from the surface [5]. In that case, direct impact ionization of the gas by beam electrons can partially neutralize the beam, causing it to over-focus, thereby spoiling the data, if not destroying the target.

The purpose of this note is to review some of the fundamental physics of electron beam heating in order to provide some elementary guidance for design of these imaging experiments to avoid overheating the target. Some specific examples for materials that we often use for imaging targets and beam-target experiments are provided.

## II. THEORY AND ESTIMATES

### *A. Short-Pulse Electron-Beam Heating*

The target is heated by beam energy deposition. The immediate increase in temperature resulting from instantaneous energy deposition in a material with no phase transitions is

$$\Delta T = \frac{\Delta E}{MC} \quad , \tag{1}$$

where $\Delta E$ is the energy deposited in the mass $M$ having specific heat $C$.

Consider heating of a range-thin foil with thickness $\delta x$ by a short pulse beam normal to the target with uniform current density $j$. By "range-thin" we mean that the thickness is much less than the range of an electron; $\delta x << R_{CSDA}$ (see Section C). By "short pulse" we mean that the beam pulse duration is too short for hydrodynamic expansion, or significant thermal conductive cooling to occur. In this case, the energy is

deposited uniformly, the process is rapid enough to be isochoric, and the appropriate specific heat to use in Eq. (1) is the specific heat at constant volume $C_V$. The isochoric specific heat $C_V$ is less than the isobaric specific heat $C_P$, which is the value most often found in tables. The difference is given by $C_V - C_P = \alpha^2 VT / \kappa_c$, where $\alpha$ is the volumetric coefficient of thermal expansion and $\kappa_c$ is the isothermal compressibility. Therefore, using the specific heat read from a table can underestimate the temperature excursion. However, since most metals have a Debye temperature at about room value, a useful approximation is that the isochoric specific heat is given by the Dulong-Petit law value of 6 cal/mol-K. Moreover, since specific heats are increasing functions of temperature, using tabular isobaric values can give useful estimates.

Energy is deposited in the material by the beam electrons. The energy lost by an electron in a given distance is macroscopically quantified by a "stopping power," usually expressed in units of energy/(areal mass density). Electron energy is lost by inelastic (ionizing) collisions with atomic electrons, and by losing energy to radiation [1]. The total stopping power is the sum of the collisional and radiative stopping powers. The radiative stopping power is the energy lost from beam electrons into bremsstrahlung radiation. Typical values of the collisional stopping power are listed in Table 1 [1]. The collisional stopping power is a weak function of energy, varying by less than 15% from 1 MeV to 30 MeV for graphite, and similarly for other materials.

Table I. Collisional stopping power of various materials

| **Material** | **dE/d(ρx) @ 15 MeV MeV/(g/cm²)** | **dE/d(ρx) @ 20 MeV MeV/(g/cm²)** |
|---|---|---|
| Be | 1.602 | 1.623 |
| Graphite | 1.787 | 1.816 |
| Al | 1.676 | 1.704 |
| Ti | 1.555 | 1.584 |
| SiO2 | 1.749 | 1.779 |
| StSt | 1.529 | 1.560 |
| Cu | 1.482 | 1.513 |
| Ta | 1.254 | 1.285 |
| W | 1.247 | 1.277 |

Since only an insignificant fraction of the bremsstrahlung is recaptured in a range-thin slab, the target heating is essentially due only to the collisional energy loss (beam-electron collisions with material electrons). Thus, the energy deposited in the foil by $N_e$ electrons is given by

$$\Delta E = N_e \left[ \frac{dE}{d(\rho x)} \right]_{coll} (\rho \, \delta x) \qquad (2)$$

where the number of electrons in a pulse length $\tau$ and area $A$ is $N_e = jA\tau / q_e$. (For a uniform current distribution, the area is calculated from the edge radius, and for a Gaussian it is calculated from the rms radius with $j$ being the peak.) In Eq. (2) we must also remember to convert the stopping power from MeV/(gm/cm$^2$) to Joules/(gm/cm2) by multiplying by $q_e$, so the electronic charge cancels out of the equation. Since the mass is just $M = \rho A \delta x$, Eq. (1) reduces to

$$\Delta T = \left[ \frac{dE}{d(\rho x)} \right]_{coll} \frac{j\tau}{C_V} \tag{3}$$

This equation exactly gives the temperature rise in Kelvins if the following units are used: the collisional stopping power is in MeV/(gm/cm$^2$), the current density $j$ is in kA/cm$^2$, the pulse length $\tau$ is in ns, and the specific heat at constant volume $C_V$ is in Joules/(gm-Kelvin).

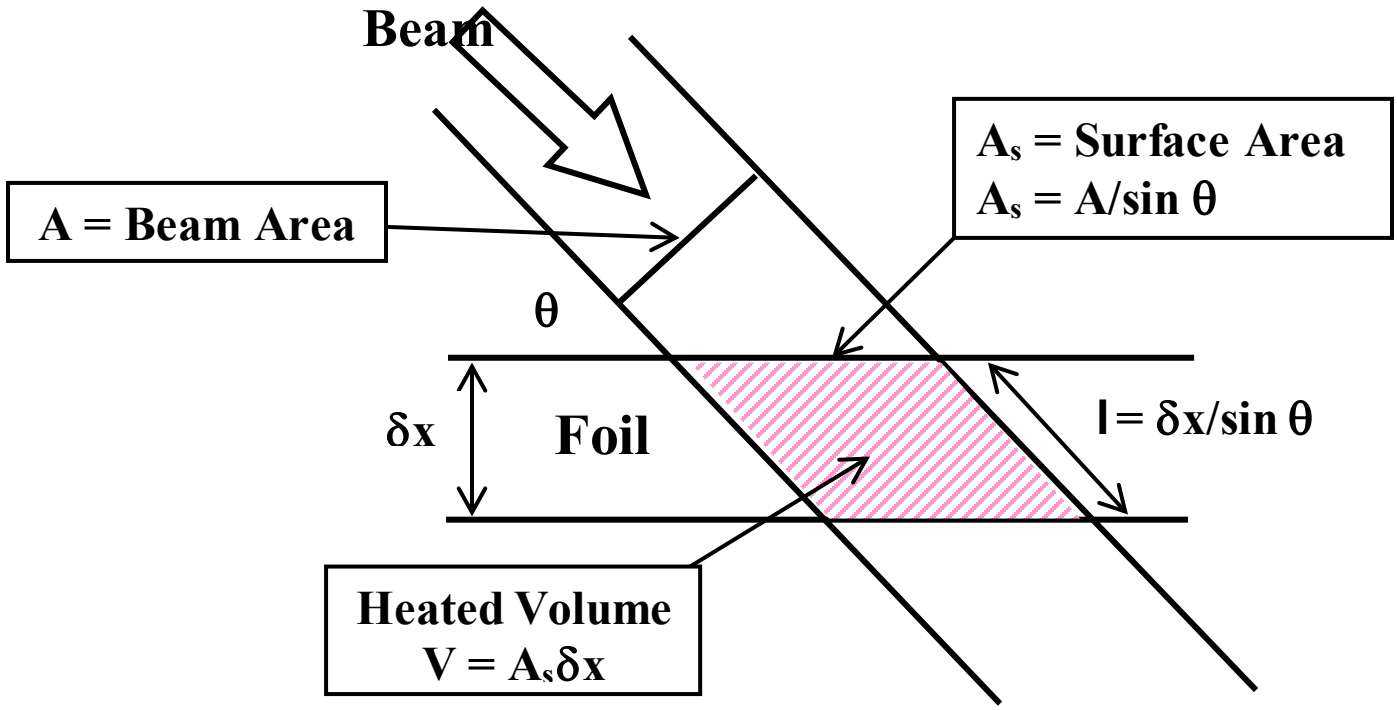


*Figure 1: Beam heating of a material slab with thickness $\delta x$*

Even if the beam is not normal to the surface Eq. (3) gives the correct temperature rise. To see this, refer to Figure 1, which illustrates the case of a beam incident at an angle $\theta \neq 90°$. It is seen that the beam deposits energy over a path length $\ell = \delta x / \sin\theta$, so the material energy increment is now

$$\Delta E = N_e \left[ \frac{dE}{d(\rho x)} \right]_{coll} (\rho\, \ell) = N_e \left[ \frac{dE}{d(\rho x)} \right]_{coll} (\rho\, \delta x / \sin\theta) \tag{4}$$

The irradiated volume of material heated is $V = A_s \delta x = A \delta x / \sin\theta$ . So, putting it all together, the $\sin\theta$ s cancel out, as do the areas, the $\delta x$ s, the $\rho$ s, and the $q_e$ s as before, leaving the same simple expression, Eq. (3).

Simply put, although the irradiated area is increased by tilting the foil, the path length, and hence energy deposition, is increased by exactly the same factor. Thus, the energy deposition per unit volume is the same as for an un-tilted foil.

Even if a low-energy, high-emittance beam is focused to a very small spot on a thin target, Eq. (3) gives a good estimate of the heating. This is because the electrons will traverse the thin foil at very low angles of incidence, even for high emittance focused to small spot. For example, consider a 2-MeV ( $\gamma = 4.914$ , $\beta\gamma = 4.811$ ) beam with 1,000 mm-mr normalized emittance focused to a 1-mm rms radius spot. The rms angle of incidence is estimated from $\varepsilon_n = 4\beta\gamma R_{rms}\theta_{rms}$ ; thus, $\theta_{rms} = 52$ mr th_rms=52 mr, or only ~ 3 degrees, and the slightly increased path length causes negligible additional heating.

Finally, we note that Eq. (3) can be used to calculate the surface heating of range-thick targets if the pulse-length is short enough that thermal diffusion is insignificant. This follows from envisioning a thick target as layers of range-thin slabs connected by thermal conductivity to each other and to cold sinks. The requirements for validity of this ansatz will be discussed next.

*B. Conductive Cooling and Diffusion*

A simple estimate of the time constant for thermal conductive cooling can be gotten from the thermal diffusion equation

$$\frac{\partial T}{\partial t} = \chi \nabla^2 T + Q \tag{5}$$

Here the thermal diffusivity is $\chi = \kappa / (\rho C_p)$, where $\kappa$ is the thermal conductivity. This equation is nonlinear, since the thermal conductivity and specific heat are functions of temperature. The last term in this equation is a source term, which can be derived from Eq. (3). The thermal constants for several materials are given in Table II. A thermal equilibration time for a given volume of material can be derived from Eq. (8) by considering a source that is a delta function of time and space in the center of an infinite volume of isotropic material. In this case the solution to Eq. (8) is

$$T(r,t) = \frac{Q}{(4\pi\chi t)^{3/2}} \exp\left( -\frac{r^2}{4\chi t} \right) \tag{6}$$

From this one can define a characteristic time for temperature to equilibrate in a given volume

$$\tau_{eq} = \frac{1}{4\chi}\left[\frac{3V}{4\pi}\right]^{2/3} \tag{7}$$

Since $\tau_{eq} \propto 1/\chi$, it is clear from Table II that copper equilibrates the fastest and titanium the slowest of all the metals. CVD diamond is the best of all.

Table II. Material Thermal Constants at 300K

| **Material** | $\kappa$ **W/(cm K)** | $\rho$ **gm/cm$^3$** | $C$ **J/(gm K)** | $\chi$ **cm$^2$/s** |
|---|---|---|---|---|
| Be | 2.00 | 1.85 | 1.83 | 0.5908 |
| Graphite (ATJ) | 1.60 | 1.9 | 0.71 | 1.1861 |
| Graphite (pyro $\|\|$c) | 0.057 | 1.9 | 0.71 | 0.0423 |
| Graphite (pyro $\perp$c) | 20.00 | 1.9 | 0.71 | 14.8258 |
| Graphite (PGS pyro) | 16.00 | 2.1 | 0.71 | 10.73 |
| CVD Diamond (25C) | 2000 | 3.52 | 0.52 | 1092 |
| CVD Diamond (500C) | 730 | 3.52 | 0.52 | 393 |
| Al | 2.37 | 2.69 | 0.90 | 0.9789 |
| Ti | 0.22 | 4.51 | 0.53 | 0.0920 |
| SiO2 | 0.0136 | 2.65 | 0.79 | 0.0065 |
| StSt | 0.86 | 7.87 | 0.45 | 0.2428 |
| Cu | 4.13 | 8.96 | 0.39 | 1.1819 |
| | | | | |
| Ta | 0.58 | 16.65 | 0.14 | 0.2488 |
| W | 1.74 | 19.35 | 0.13 | 0.6917 |

Table III gives the equilibration times for various volumes of impulsively heated material. With one exception, these are much longer than the beam pulse, so thermal conductivity is not expected to have a significant effect on energy deposition by beam heating.

The exception might be Pyrolytic graphite, so it is instructive to consider heating of a thin foil in more detail. A 1-cubic mm volume in an infinite isotropic medium with the fast thermal conductivity and density of these foils would take about 90 microseconds to relax to room temperature. Therefore, even though it's fast, it is slow compared to the <100 ns energy deposition time and would not be expected to effect the local temperature rise due to e-beam heating during a single pulse.

Table III. Thermal Equilibration Time in seconds for various volumes

| Material | V=1 mm$^3$ s | V=10 mm$^3$ s | V=100 mm$^3$ s | V=1 cm$^3$ s |
|---|---|---|---|---|
| Be | 1.63E-03 | 7.56E-03 | 3.51E-02 | 0.162845 |
| Graphite (ATJ) | 8.11E-04 | 3.76E-03 | 1.75E-02 | 8.11E-02 |
| Graphite (pyro $\|\|$c) | 2.27E-02 | 1.06E-01 | 4.90E-01 | 2.27 |
| Graphite (pyro $\perp$c) | 6.49E-05 | 3.01E-04 | 1.40E-03 | 6.49E-03 |
| Graphite (PGS pyro) | 8.97E-05 | 4.16E-04 | 1.93E-03 | 8.97E-03 |
| Al | 9.83E-04 | 4.56E-03 | 2.12E-02 | 0.098282 |
| Ti | 1.05E-02 | 4.85E-02 | 2.25E-01 | 1.045747 |
| SiO2 | 1.48E-01 | 6.87E-01 | 3.19E+00 | 14.80134 |
| StSt | 3.96E-03 | 1.84E-02 | 8.54E-02 | 0.396247 |
| Cu | 8.14E-04 | 3.78E-03 | 1.75E-02 | 0.081402 |
| Ta | 3.87E-03 | 1.79E-02 | 8.33E-02 | 0.386691 |
| W | 1.39E-03 | 6.46E-03 | 3.00E-02 | 0.13909 |

*C. Other approximations*

*1. Stopping power and range*

In the continuous slowing down approximation (CSDA) the range $R_{CSDA}$ in cm is

$$R_{CSDA} = \frac{1}{\rho}\int_{KE}^{0}\left[\frac{dE}{d(\rho x)}\right]^{-1} dE \tag{8}$$

Here, $dE/d(\rho x)$ is the total stopping power in MeV/(gm/cm$^2$), $KE$ is the initial beam kinetic energy in MeV, and $\rho$ is the material density in gm/cm$^3$. It is worth noting that the collisional stopping power is only weakly dependent on the atomic number of the material. Therefore, heating is almost entirely a function of the material heat capacity. Moreover, at the beam energies of interest, the collisional stopping power is only weakly dependent on energy. For example, the stopping power for carbon varies by only ~5% between 10 MeV and 25 MeV. CSDA range values for many materials are included in ref. [1].

*2. Heat of fusion, vaporization, and other phase transitions*

Eq. (3) is enough to describe the heating of a target by large, nondestructive beams; for example, in many cases of beam imaging. On the other hand, for radiography, the beam is focused to the smallest possible spot, which ensures destruction of the converter. In this case, one must take the heat of phase transitions into account, and Eq. (3) replaced by

$$\Delta T = \frac{1}{C_V}\left\{ j\tau \left[ \frac{dE}{d(\rho x)} \right]_{coll} - \sum_k \Delta H_k \right\} \tag{9}$$

where the $\Delta H_k$ are the specific heats associated with the various phase transitions (fusion, vaporization, dissociation, etc.). Table IV lists these for our candidate materials. The heat associated with melting is usually much less than that associated with vaporization, which can amount to 10%-20% of the beam energy deposition.

Table IV Heat of Phase Transitions

| **Material** | **Molar Volume $cm^3$/Mole** | **$T_m$ K** | **$\Delta H_m$ kJ/mole (melt)** | **$\Delta H_m$ kJ/g** | **$T_v$ K** | **$\Delta H_v$ kJ/mole (vaporization)** | **$\Delta H_v$ kJ/g** |
|---|---|---|---|---|---|---|---|
| Be | 4.85 | 1287 | 13 | 2471 | 2471 | 291 | 60.00 |
| Graphite | | | | 4200 | 4200 | | |
| CVD Diamond | | 1773 | | | | | |
| Al | 10.00 | 660 | 10.8 | 2520 | 2520 | 293 | 29.30 |
| Ti | 10.64 | 1608 | 15.1 | 3287 | 3287 | 410 | 38.53 |
| SiO2 | | | | | | | |
| StSt | 7.09 | 1538 | 13.8 | 2872 | 2872 | 350 | 49.37 |
| Cu | 7.11 | 1083 | 13 | 2543 | 2543 | 302 | 42.48 |
| | | | | | | | |
| Ta | 10.85 | 2996 | 35 | 5350 | 5350 | 745 | 68.66 |
| W | 9.47 | 3420 | 35.1 | 5680 | 5680 | 770 | 81.31 |

From Eq. 6 the time needed to burn through a particular phase transition is simply

$$\tau(ns) = \frac{\Delta H_k}{j\left[ \frac{dE}{d(\rho x)} \right]_{coll}} \tag{10}$$

where the units are the same as in the heating calculation, and the latent heat is in J/g.

*3. Radiative Cooling*

Radiative cooling from the heated surface is

$$P / A = \sigma T^4 \tag{11}$$

where $\sigma = 5.67 \times 10^{-8} \left( \mathrm{W/m^2} \right) / \mathrm{K}^4$ is the Stefan-Boltzmann constant. Although important after the end of the beam pulse, this has little effect on the temperature excursion. For

example, at the tantalum melt temperature (2996K) the rate of cooling by radiation from a 1-mm FWHM spot is ~4 W, compared with ~2.4 TW beam heating power.

*4. Hydrodynamics*

Hydrodynamics of the isochorically heated volume and its nearby surroundings by unfocused beams is unlikely to have much influence on temperature rise, because shock and sound velocities are of order cm/micro-sec, and material motion is negligible over the few tens of ns beam pulses. However, it is complicated for focused beams by the fact that temperature and density are squarely in the warm dense matter regime, where the EOS is uncertain.

References


[1] M. Burns, B. Carlsten, H. Davis, C. Ekdahl and et al., "Status of the DARHT phase-2 long-pulse accelerator," in *Part. Accel. Conf.*, Chicago, IL, USA, 2001.

[2] C. Ekdahl and e. al., "First beam at DARHT-II," in *Part. Accel. Conf.*, 2003.

[3] C. Ekdahl, E. O. Abeyta, H. Bender, W. Broste, C. Carlson, L. Caudill, K. C. D. Chan, Y.-J. Chen, D. Dalmas, G. Durtschi, S. Eversole, S. Eylon, W. Fawley, D. Frayer, R. Gallegos, J. Harrison, E. Henestroza, M. Holzscheiter, T. Houck, T. Hughes, S. Humphries, D. Johnson, J. Johnson, K. Jones, E. Jacquez, B. T. McCuistian, A. Meidinger, N. Montoya, C. Mostrom, K. Moy, K. Nielsen, D. Oro, L. Rodriguez, P. Rodriguez, M. Sanchez, M. Schauer, D. Simmons, H. V. Smith, J. Studebaker, R. Sturgess, G. Sullivan, C. Swinney, R. Temple, C. Y. Tom and S. S. Yu, "Initial electron-beam results from the DARHT-II linear induction accelerator," *IEEE Trans. Plasma Sci.,* vol. 33, no. 2, pp. 892 - 900, 2005.

[4] C. Ekdahl and et al., "Emittance growth in the DARHT-II linear induction accelerator," *IEEE Trans. Plasma Sci.,* vol. 45, no. 11, pp. 2962 - 2973, Nov 2017.

[5] C. Vermare, H. A. Davis, D. C. Moir and T. P. Hughes, "Ion emission from solid surfaces induced by intense electron beam impact," *Phys. Plasmas,* vol. 10, no. 1, pp. 277 - 284, Jan. 2003.

[6] M. L. Berger and et al., "Stopping-power and range tables for electrons, protons, and helium ions," NIST, July 2017. [Online]. Available: https://www.nist.gov/pml/stopping-power-range-tables-electrons-protons-and-helium-ions. [Accessed March 2021].